Int. J. Heat Mass Transfer. Vol. 17, pp. 1465–1474. Pergamon Press 1974. Printed in Great Britain

FREE CONVECTION OVER A VERTICAL POROUS PLATE WITH TRANSPIRATION

P. G. PARIKH, R. J. MOFFAT, W. M. KAYS and D. BERSHADER

Departments of Mechanical and Aerospace Engineering,
Stanford University, Stanford, California 94305, U.S.A.

(*Received* 3 *January* 1974)

Abstract—The problem of free convection over an isothermal vertical porous plate with transpiration is studied in this paper both numerically and experimentally. The effects of uniform transpiration on heat transfer and temperature and velocity profiles are predicted. Experimental data on non-dimensional temperature profiles for values of streamwise variable

$$\xi \triangleq \frac{v_0 x}{\nu}\left(\frac{4}{Gr_x}\right)^{1/4}$$

in the range $-2 \leqslant \xi \leqslant 2$, obtained interferometrically, show close agreement with numerical predictions. An accuracy of $\pm 1°F$ in temperature profile measurement is estimated for $(T_w - T_\infty) = 50°F$.

NOMENCLATURE

C_p, specific heat of fluid;
g, gravitational acceleration;
Gr_x, Grashof number $\dfrac{g(t_w - t_\infty)x^3}{\nu^2 T_\infty}$;
h_x, heat-transfer coefficient;
i, enthalpy of the fluid;
k, thermal conductivity of fluid;
L, light path length;
$\dot{m}_0''$, mass flux at the wall;
Nu_x, Nusselt number $\dfrac{h_x X}{k}$;
Pr, Prandtl number $= \nu/\alpha$;
$\dot{q}_0''$, heat flux (conductive) at the wall;
S, fringe shift;
t, T, temperature;
u, velocity component in x-direction;
v, velocity component in y-direction;
v_0, transpiration velocity at the wall;
x, streamwise co-ordinate (along the plate);
y, cross-stream co-ordinate (normal to the plate).

Greek letters

α, thermal diffusivity;
β, coefficient of volume expansion;
θ, nondimensional temperature $\dfrac{t - t_\infty}{t_w - t_\infty}$;
λ, wave length of monochromatic light;
μ, absolute viscosity of fluid;
ν, kinematic viscosity of fluid;
ξ, streamwise nondimensional variable;
ρ, density of fluid;
ψ, stream function.

Subscripts

0, w, wall condition;
∞, ambient fluid condition.

INTRODUCTION

THE EFFECTS of transpiration on free convection flow over a vertical porous plate has been the subject of several investigations. Eichhorn [1] found conditions on the transpiration rates and wall temperature under which self-similar solutions are possible for this case. Sparrow and Cess [2] presented approximate series solutions for the case of uniform transpiration and wall temperature. More recently, Merkin [3] gave numerical solutions to the boundary-layer equations for Prandtl number of 1·0 and discussed the asymptotic behavior for large transpiration rates. All these investigators presented analysis for a constant property fluid in which density variations are retained only in the body force term of the momentum equation. Clarke [4] analyzed the problem with density variations in full and presented solutions for the outer region of the flow field for blowing conditions under which self similar solutions to the boundary-layer equations obtain. On the experimental side, to our knowledge, there is only one investigation reported in the available literature on the subject. Brdlik and Mochalov [5] have studied the problem using interferometry for small values of blowing and suction. In the present investigation, numerical solutions to the boundary-layer equations for uniform transpiration and wall temperature case

have been obtained not only retaining density variations in full, but also taking into account variations in the properties μ, κ and c_p. These numerical predictions are then compared with experimental data obtained interferometrically for values of nondimensional streamwise variable

$$\xi = \frac{v_0 x}{\nu}\left(\frac{4}{Gr_x}\right)^{1/4}$$

in the range $-2 \leqslant \xi \leqslant 2$.

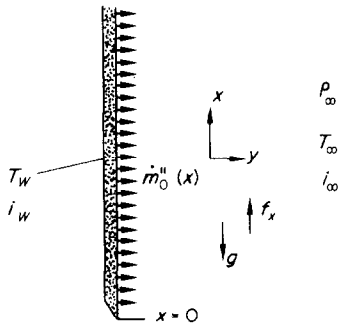

FIG. 1. The coordinate system.

BOUNDARY-LAYER EQUATIONS

Neglecting viscous dissipation in the energy equation but retaining variations in properties ρ, κ, μ and c_p, the equations of the steady free convection boundary layer on a vertical porous plate with coordinates as shown in Fig. 1 are:

mass: $$\frac{\partial(\rho u)}{\partial x}+\frac{\partial(\rho v)}{\partial y}=0$$

x-momentum: $$\rho u\frac{\partial u}{\partial x}+\rho v\frac{\partial u}{\partial y}=f_x+\frac{\partial}{\partial y}\left(\mu\frac{\partial u}{\partial y}\right) \quad (1)$$

energy: $$\rho u\frac{\partial i}{\partial x}+\rho v\frac{\partial i}{\partial y}=\frac{\partial}{\partial y}\left(\kappa\frac{\partial t}{\partial y}\right)$$

equations of state: $$i=i(t);\quad \rho=\rho(t,p);$$
$$\mu=\mu(t);\quad \kappa=\kappa(t).$$

Here, f_x is the force of buoyancy per unit volume of a fluid element and is given as

$$f_x = g(\rho_\infty - \rho).$$

The boundary conditions are:

$$u=0,\quad i=i_w,\quad (pV)=\dot{m}_0''(x)\quad \text{at}\quad y=0,\quad x>0$$
$$u\to 0,\quad i\to i_\infty\quad \text{as}\quad y\to\infty \quad (2)$$
and
$$u=0,\quad i=i_\infty\quad \text{at}\quad x=0,\quad y>0.$$

The problem solved numerically in this paper is the one posed by the set of equations (1) together with boundary conditions (2) for the case of $i_w = \text{const}$ ($i_w > i_\infty$) and $\dot{m}_0'' = \text{const}$.

CONDITIONS FOR SELF SIMILARITY

Before discussing the numerical solution procedure it is worthwhile to consider the conditions under which self similar solutions exist. If density variations are disregarded except in the body force term and the properties μ, κ, c_p and β are constants, then equations (1) become:

mass: $$\frac{\partial u}{\partial x}+\frac{\partial v}{\partial y}=0$$

x-momentum: $$u\frac{\partial u}{\partial x}+v\frac{\partial u}{\partial y}=g\frac{(t_w-t_\infty)\theta}{T_\infty}+\nu\frac{\partial^2 u}{\partial y^2} \quad (3)$$

energy: $$u\frac{\partial\theta}{\partial x}+v\frac{\partial\theta}{\partial y}=\alpha\frac{\partial^2\theta}{\partial y^2}$$

where

$$\theta \triangleq \frac{t-t_\infty}{t_w-t_\infty}$$

and the coefficient of volume expansion β is replaced by $1/T_\infty$.

The boundary conditions are:

$$u=0,\quad \theta=1,\quad v=v_0(x)\quad \text{at}\quad y=0,\quad x>0$$
$$u\to 0,\quad \theta\to 0\quad \text{as}\quad y\to\infty \quad (4)$$
$$u=0,\quad \theta=0\quad \text{at}\quad x=0,\quad y>0.$$

If the governing equations and the boundary conditions of this problem are examined for invariance under a group of affine transformations, possibility of the existence of self similar solutions is revealed provided

$$v_0 \sim x^{-1/4}.$$

Introducing the similarity variable

$$\eta \triangleq \frac{y}{x}\left(\frac{Gr_x}{4}\right)^{1/4}$$

where

$$Gr_x \triangleq \frac{g(T_w-T_\infty)x^3}{\nu^2 T_\infty}$$

is the Grashof number and the stream function

$$\psi = 4\nu\left(\frac{Gr_x}{4}\right)^{1/4}\zeta(\eta) \quad (5)$$

leads to the following set of coupled ordinary differential equations and boundary conditions:

$$\zeta''' + 3\zeta\zeta'' - 2(\zeta')^2 + \theta = 0$$

and

$$\theta'' + 3Pr\zeta\theta' = 0.$$

Boundary conditions:

$$\zeta'(\eta)=0,\quad \theta=1,\quad \zeta(\eta)=-M/3\quad \text{at}\quad \eta=0$$
$$\theta\to 0,\quad \zeta'(\eta)\to 0\quad \text{as}\quad \eta\to\infty. \quad (6)$$

Here the blowing parameter M is defined as:

$$M \triangleq \frac{v_0 x}{\nu}\left(\frac{4}{Gr_x}\right)^{1/4}, \quad v_0 \sim x^{-1/4}.$$

The similarity solutions for ζ and θ with M as a parameter are given by Eichhorn [1] and by Ostrach [6] for $M = 0$ (zero blowing case).

If, however, v_0 is a constant, self-similar solution is not possible. In this case x and y are replaced by new independent variables η and ξ defined as

$$\eta \triangleq \frac{y}{x}\left(\frac{Gr_x}{4}\right)^{1/4}; \quad \xi \triangleq \frac{v_0 x}{\nu}\left(\frac{4}{Gr_x}\right)^{1/4}, \quad v_0 = \text{const.} \quad (7)$$

The transformed problem, after introduction of the stream function as defined in equation (5) becomes:

$$\frac{\partial^3\zeta}{\partial\eta^3} + 3\zeta\frac{\partial^2\zeta}{\partial\eta^2} - 2\left(\frac{\partial\zeta}{\partial\eta}\right)^2 + \theta = \xi\left[\frac{\partial\zeta}{\partial\eta}\frac{\partial^2\zeta}{\partial\eta\,\partial\xi} - \frac{\partial\zeta}{\partial\xi}\frac{\partial^2\zeta}{\partial\eta^2}\right]$$
$$\frac{1}{Pr}\frac{\partial^2\theta}{\partial\eta^2} + 3\zeta\frac{\partial\theta}{\partial\eta} = \xi\left[\frac{\partial\zeta}{\partial\eta}\frac{\partial\theta}{\partial\xi} - \frac{\partial\theta}{\partial\eta}\frac{\partial\zeta}{\partial\xi}\right]. \quad (8)$$

Boundary conditions:

$$\frac{\partial\zeta}{\partial\eta} = 0, \quad \theta = 1 \quad \text{and} \quad \zeta = -\xi/4 \quad \text{at} \quad \eta = 0$$

and

$$\frac{\partial\zeta}{\partial\eta} \to 0, \quad \theta = 0 \quad \text{as} \quad \eta \to \infty.$$

Finite difference solution to this problem using a slightly modified form of the stream function (to give a homogeneous boundary condition on ζ) is given by Merkin [3] for $Pr = 1$ and an approximate series solution was presented by Sparrow and Cess [2] for $Pr = 0{\cdot}72$.

THE SOLUTION PROCEDURE

Returning now to the original problem with the governing equations (1) and boundary conditions (2), the numerical solution presented here accounts not only for variations of density, but also for other properties μ, c_p and k as given by standard tables for properties of air such as Eckert and Drake tables. The numerical procedure used was a modified version of Patankar–Spalding [7] program which has been in use at Stanford for several years.

The program uses a fully implicit finite difference procedure and solves the parabolic partial differential equations of the boundary-layer after introducing the von Mises transformation.

The program requires specification of initial profiles of velocity and enthalpy. In our case, these profiles were specified very close to the leading edge ($x = \frac{1}{4}$ in) using the values given by Ostrach's solution for an impermeable wall. It was intended, from the outset of this investigation, to compare experimental results with the predictions, hence the wall condition chosen was the one least difficult to set experimentally: constant mass flux and constant temperature at the wall. Although the program is capable of taking into account variations of properties associated with large temperature difference ($t_w - t_\infty$), the calculations and the experiment were both conducted using only a 50 degF difference to permit comparisons of these results with the available constant property solutions. The program prints out results in dimensional form such as temperature in degF and velocity in ft/s as functions of x and y in feet. However, results are presented here in non-dimensional form using values of ν and k based on the average temperature between the wall and the free-stream. The normal velocity at the wall was computed from the known mass flux by using the density at the wall.

Discussion of numerical results

The non-dimensional temperature and velocity profiles predicted by the program for the zero blowing

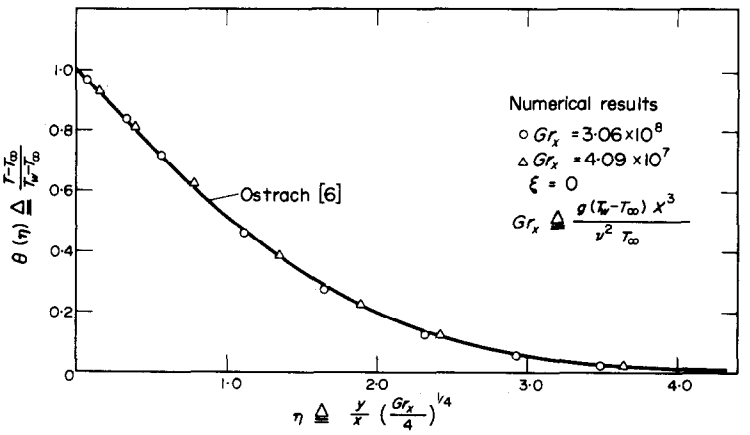

FIG. 2(a). Non-dimensional temperature profile.

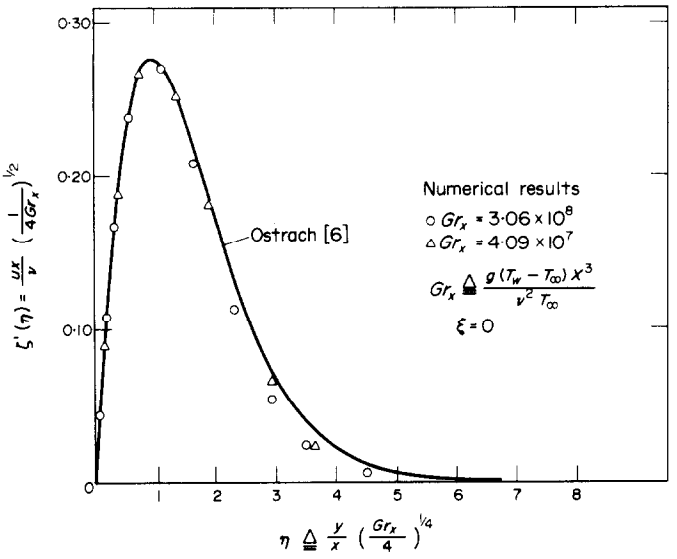

FIG. 2(b). Non-dimensional velocity profile.

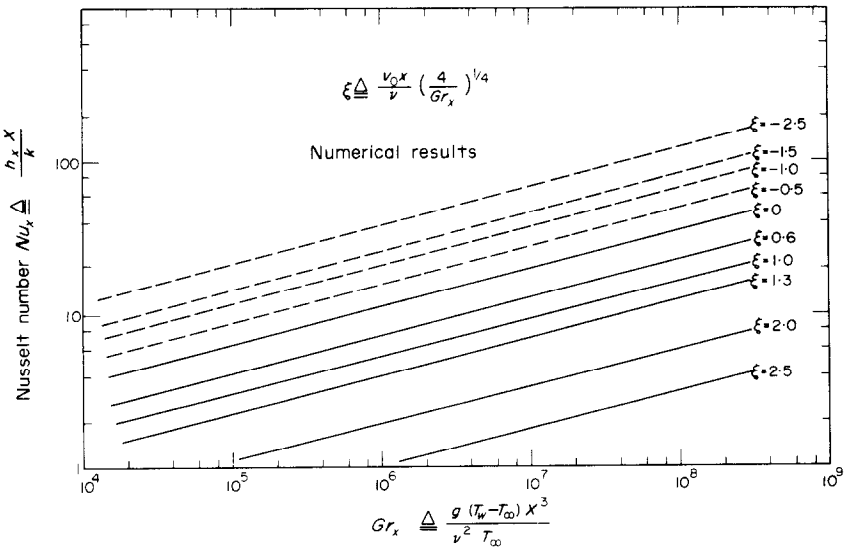

FIG. 3. Effect of transpiration on Nusselt number.

case ($\xi = 0$) are compared in Figs. 2(a), (b) with Ostrach's [6] solutions. Numerical results for two Grashof numbers are shown and agreement is seen to be excellent. The slight departures in the velocity profile are assumed to result from the use of variable properties in our solutions.

The effect of transpiration on heat-transfer rate from the wall is shown in Fig. 3. At a given Grashof number, blowing decreases while suction increases the heat transfer rate. All constant ξ lines have the same slope on a log–log plot of Nu_x vs Gr_x which may be explained as follows: We have

$$\dot{q}_0'' = -k\left(\frac{\partial t}{\partial y}\right)_{y=0} = -\frac{k}{x}(T_w - T_\infty)\left(\frac{Gr_x}{4}\right)^{1/4}\left(\frac{\partial \theta}{\partial \eta}\right)_{\eta=0}.$$

Defining a heat-transfer coefficient h_x

$$\dot{q}_0'' = h_x(T_w - T_\infty).$$

Therefore the Nusselt number

$$Nu_x \triangleq \frac{h_x x}{k} = -\left(\frac{Gr_x}{4}\right)^{1/4}\left(\frac{\partial \theta}{\partial \eta}\right)_{\eta=0}$$

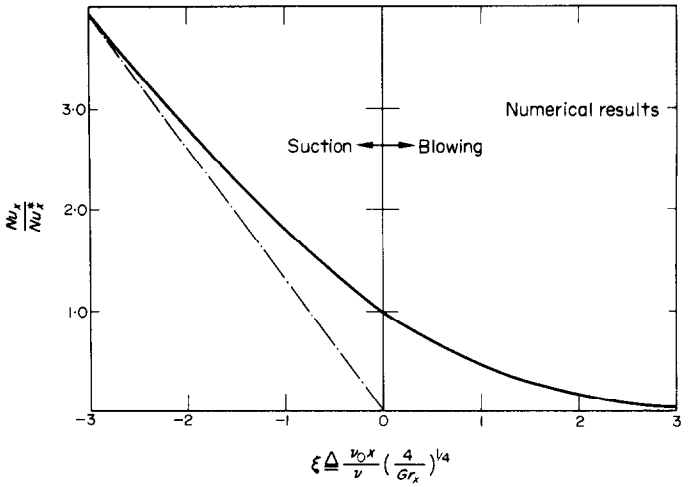

FIG. 4. Effects of transpiration on Nusselt number at a fixed Grashof number.

Let

$$\left.\frac{\partial\theta}{\partial\eta}\right)_{\eta=0} = f(\xi).$$

Then

$$Nu_x = -\left(\frac{Gr_x}{4}\right)^{1/4} f(\xi). \tag{9}$$

This shows that on a log–log plot of Nu_x vs Gr_x, all constant ξ lines have the same 1/4 slope.

Next, let Nu_x^* denote zero blowing condition. Then from (9),

$$\frac{Nu_x}{Nu_x^*} = \frac{f(\xi)}{f(0)}. \tag{10}$$

The change in the Nusselt number at a given Grashof number due to transpiration as given by equation (10) is shown in Fig. 4 and tabulated in Table 1. On the blowing side, $Nu_x \to 0$ as $\xi \to \infty$ showing that conductive heat transfer at the wall drops to zero as blowing is increased indefinitely. On the suction side, the curve approaches an asymptote. This asymptotic suction behavior will be discussed next.

Table 1

ξ	Nu_x/Nu_x^*
−2·4	3·245
−2·0	2·820
−1·6	2·395
−1·2	1·990
−1·0	1·805
−0·8	1·625
−0·4	1·300
0·0	1·000
0·4	0·755
0·8	0·550
1·0	0·465
1·2	0·380
1·6	0·260
2·0	0·160
2·4	0·085

For large suction rates, temperature and velocity become independent of x [3]. Dropping derivatives with respect to x in the continuity and energy equations and solving for θ, we arrive at the asymptotic suction profile for temperature, given by the exponential function

$$\theta = \exp\left[\frac{v_0}{\alpha} y\right] = \exp[Pr\xi\eta]. \tag{11}$$

Therefore

$$\left.\frac{\partial\theta}{\partial\eta}\right)_{\eta=0} = Pr\xi = f(\xi)$$

$$\frac{Nu_x}{Nu_x^*} = \frac{f(\xi)}{f(0)} = \frac{Pr}{f(0)}\xi. \tag{12}$$

Thus, in the asymptotic suction limit, a plot of Nu_x/Nu_x^* vs ξ approaches an asymptote with a slope $Pr/f(0)$. Using $Pr = 0{\cdot}7$ and $f(0) = -0{\cdot}5048$ from our numerical solution, we get a slope of $-1{\cdot}39$ which agrees with the slope of the asymptote in Fig. 4 within 2 per cent.

In the asymptotic suction limit, equation (11) shows that

$$\dot{q}_0'' = -k\left.\frac{\partial t}{\partial y}\right)_{y=0} = \frac{kv_0}{\alpha}(T_w - T_\infty) = \rho c_p v_0 (T_w - T_\infty).$$

Thus, all the heat transferred from the wall goes into heating the sucked air from free-stream to wall temperature and none is convected downstream in the boundary layer.

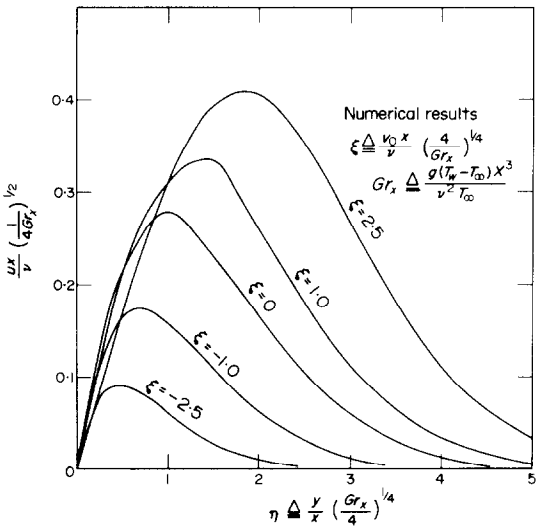

FIG. 5. Non-dimensional velocity profiles.

Fig. 7 for one fixed value of ξ and three different Gr_x and $\dot{m}''_0$. All points fall on the same curve, providing a check on the accuracy of computed results. The non-dimensional temperatures are tabulated as functions of η and ξ in Table 2.

EXPERIMENTAL SET-UP

The objective of the experimental part of this investigation was to obtain nondimensional temperature profiles for several values of ξ and Grashof numbers.

The porous plate test section used here was designed for interferometric studies of transpired boundary layers. It consists of four 6 × 4 in sintered bronze porous plates of $\frac{1}{4}$-in thickness, supported on an aluminum casting by means of thin phenolic strips glued to their sides. The test surface is 16-in long and 6-in wide providing an optical path length of 6 in. The plates were heated by resistance wires glued into grooves on the underside of the plates. Power was supplied to each segment individually. The plate temperatures were

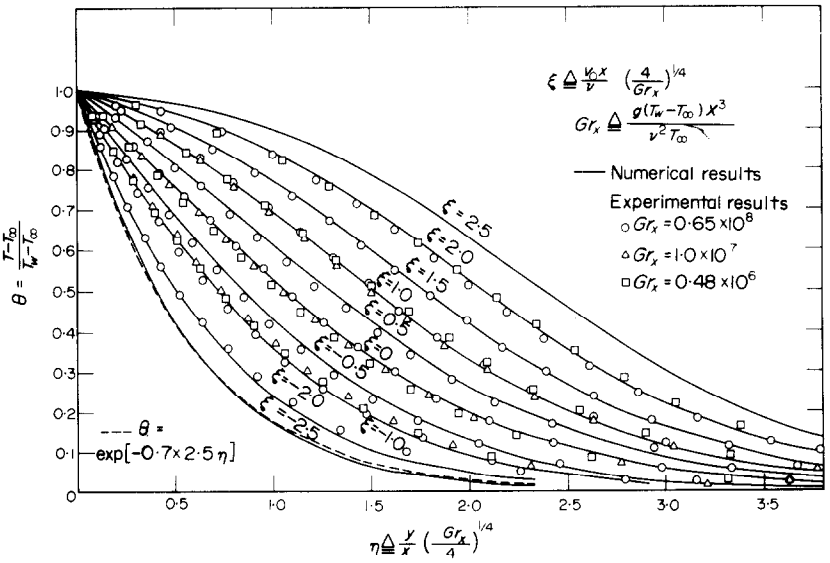

FIG. 6. Non-dimensional temperature profiles.

The predicted nondimensional velocity profiles are shown in Fig. 5. The effect of blowing is to increase the maximum velocity and shift its location farther away from the wall.

The predicted nondimensional temperature profiles are shown as solid lines in Fig. 6. As ξ, or blowing rate, increases, the temperature profiles become fuller and boundary-layer thickness increases. The exponential suction profile given by equation (11) is compared with computed results for $\xi = -2.5$ and the two curves are almost identical.

Finally, calculated values of θ are plotted vs η in

measured by a set of five iron–constantan thermocouples, one at the center and four near the edges in each plate. Uniformity of temperatures measured by these thermocouples was better than ± 1 degF for $(t_w - t_\infty) = 50$ degF. The uniformity of porosity was better than ± 5 per cent for each plate. The overall design features of the test section used here were similar to those of the test section used by Moffat [8] and its success in transpired boundary-layer studies has been well established over a period of several years.

Each of the porous plate segments was supplied individually with transpiration air through a flow

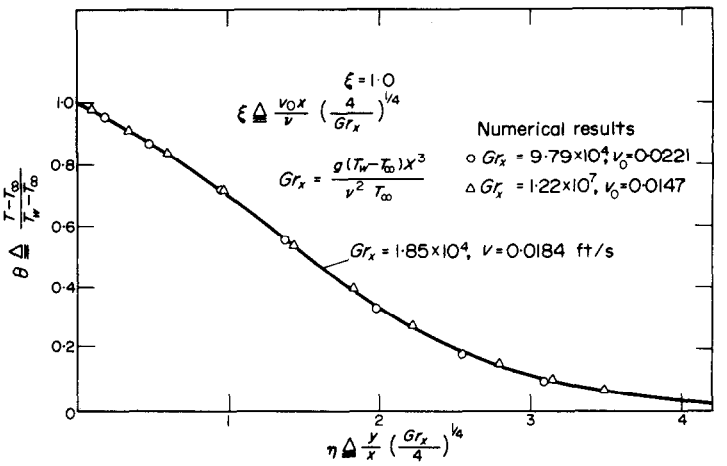

FIG. 7. Similarity of non-dimensional temperature profiles.

Table 2. Non-dimensional temperatures

η	$\theta(\eta, \xi)$							
	$\xi = -2{\cdot}0$	$-1{\cdot}0$	$-0{\cdot}5$	0·0	0·5	1·0	1·5	2·0
0	1·000	1·000	1·000	1·000	1·000	1·000	1·000	1·000
0·2	0·764	0·840	0·871	0·902	0·932	0·951	0·967	0·981
0·4	0·578	0·695	0·747	0·805	0·855	0·895	0·930	0·957
0·6	0·441	0·570	0·630	0·711	0·776	0·835	0·885	0·929
0·8	0·325	0·455	0·523	0·618	0·695	0·766	0·832	0·890
1·0	0·240	0·360	0·432	0·526	0·614	0·695	0·775	0·845
1·2	0·175	0·278	0·348	0·444	0·535	0·620	0·708	0·792
1·4	0·125	0·215	0·277	0·370	0·461	0·545	0·637	0·734
1·6	0·088	0·160	0·217	0·305	0·386	0·468	0·564	0·669
1·8	0·065	0·121	0·168	0·245	0·317	0·393	0·490	0·597
2·0	0·048	0·090	0·128	0·196	0·260	0·329	0·418	0·525
2·2	0·034	0·066	0·093	0·156	0·213	0·271	0·352	0·454
2·4	0·025	0·048	0·068	0·125	0·173	0·224	0·293	0·386
2·6		0·033	0·047	0·098	0·138	0·180	0·241	0·324
2·8		0·024	0·032	0·075	0·108	0·142	0·195	0·267
3·0			0·022	0·055	0·084	0·112	0·158	0·220
3·2				0·043	0·064	0·089	0·130	0·180
3·4				0·032	0·050	0·070	0·103	0·144
3·6				0·025	0·040	0·055	0·079	0·115
3·8				0·020	0·030	0·045	0·064	0·092
4·0				0·015	0·020	0·033	0·055	0·075

metering system. The blowing air was supplied from laboratory compressed air line, after two pressure regulators and a filter, and suction was provided by connecting the flow metering system to the inlet of a small centrifugal blower. The flow metering capability needed for this work was in the low range of 0·05–0·5 scfm and a specially designed system of flowmeters was used. Each of the flowmeters consisted of two porous disks inserted into a 6-in long 1-in dia. plastic pipe with pressure taps to measure the pressure drop across these disks. Each flowmeter was calibrated individually using a laminar flow metering element to determine its pressure drop vs flow rate characteristic and repeatability was found to be within 2 per cent.

The power supplied to each plate segment was controlled by a variac connected to line through a voltage stabilizer and measured by a wattmeter. No attempt was made to measure the local heat-transfer rate directly by accounting for energy loss from the plates. Heat transfer from a plate, (for $\xi = 0$) as computed from the measured temperature gradient at the wall, accounted for only 60–80 per cent of the total power supplied to the plate, hence any direct measurement would have been quite uncertain.

The temperature profiles were determined by a Mach–Zehnder interferometer designed and constructed at Stanford. The mirrors and beam splitters were 2 in in diameter and were supported in gimbaled

mounts with micrometer controls. A mercury light source was used with a filter to give a monochromatic light beam at 5461 Å.

The porous plate test section was suspended vertically from an adjustable steel post with leading edge of the plate at a height of 3–4 ft from the floor. The entire test section assembly was enclosed in a relatively large open ended cardboard box whose inside surface was lined with aluminized mylar. The inside surface of the box was kept at least 6 in away from the plate surface to ensure that there was neglible effect of confinement on the free convection boundary layer developing along the plate. The bottomless cardboard enclosure did not extend all the way down to the floor but left enough open area at the bottom for freely entraining surrounding air. The air conditioning and exhaust vents in the room were sealed off to avoid circulation in the room. Balsa wood fences with optical quality windows were installed on both sides of the plates to prevent lateral spreading of the boundary layer at the edges of the plate. With these precautions, exceptional steadiness of the free convection boundary layer was achieved even at Grashof numbers of 10^8 and $\xi = 2{\cdot}0$.

TEST PROCEDURE AND DATA REDUCTION

Three series of interferograms were obtained corresponding to three Grashof numbers and several values of ξ at each Grashof number (Fig. 8). The pictures with 4:1 magnification were taken with Polaroid type 57 film using three 20 ms exposures at intervals of about 5 s. The finite fringe field interferograms were taken with initial fringe orientation perpendicular to the unheated plate. The interferograms were evaluated under a traversing microscope with a magnification of ten by the method described in [9]. An accuracy of $\pm 0{\cdot}05$ fringe shift is expected in this procedure.

Careful alignment of the test plate surface with the light beam was necessary to avoid errors in measurement. This alignment was done by installing a micrometer control for the orientation of the plate and using the method of reflection interference described in [10]. The fringe focusing plane was located at the centerline of the test section to minimize refraction errors [10].

The density at a point in the boundary layer was evaluated by the Dale–Gladstone relationship

$$\rho - \rho_\infty = \frac{\lambda}{KL} S(x, y) \tag{13}$$

where K, the Dale–Gladstone constant for air was taken as $0{\cdot}226\ \text{cm}^3/\text{g}$. The temperature at the point was then calculated using perfect gas law. The wall temperature predicted by fringe shift measurements agreed with the thermocouple measured averaged temperature within ± 1 deg F.

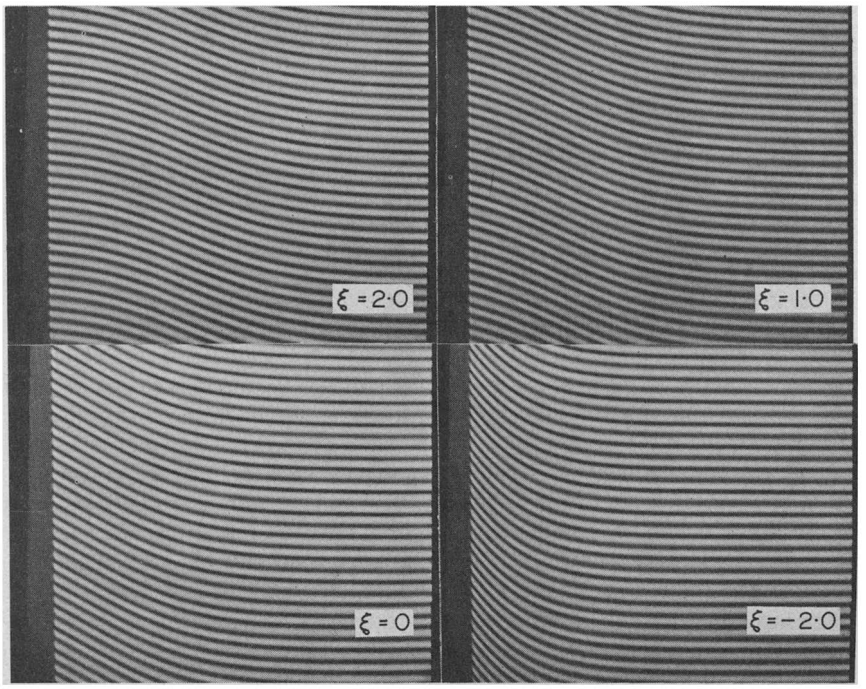

FIG. 8. Interferograms at $x = 10$ in for different transpiration rates.

EXPERIMENTAL RESULTS

The experimental data are compared with numerical predictions in Fig. 6. Property values based on average temperature between the wall and the freestream were used to express experimental results in nondimensional form. The agreement of the experimental data with the predictions of the Patankar–Spalding program is seen to be excellent. Although direct measurements of local heat-transfer rates at the wall were not made in this investigation, the numerical predictions in Figs. 3 and 4 may be relied upon, as the close agreement between theory and experiment in Fig. 6 testifies.

CONCLUSIONS

Numerical solutions to the variable property transpired free convection boundary-layer equations have been obtained using finite difference procedure of Patankar and Spalding. Interferometrically measured non-dimensional temperature profiles for the uniform wall temperature and transpiration rate case agreed closely with these numerical predictions.

Acknowledgements—The authors are indebted to Messrs. M. Pimenta and M. Crawford for their assistance in the early phase of the experimental program. This study was supported in part by the National Aeronautics and Space Administration under Grant (NASA-Ngl-05-020-134).

REFERENCES

1. R. Eichhorn, The effects of mass transfer on free convection flow, *J. Heat Transfer* **82C**, 260–263 (1960).
2. E. M. Sparrow and R. D. Cess, Free convection with blowing or suction, *J. Heat Transfer* **81C**, 387–389 (1961).
3. J. H. Merkin, Free convection with blowing and suction, *Int. J. Heat Mass Transfer* **15**, 989–999 (1972).
4. J. F. Clarke, Transpiration and natural convection–vertical flat plate problem, *J. Fluid Mech.* **57**, Part 1, 45–61 (1973).
5. P. M. Brdlik and V. A. Mochalov, Experimental study of free convection with porous blowing and suction on a vertical surface, *J. Engng Physics (Inzh.-Fiz. Z.)* **10**(1), 3–10 (1966).
6. S. Ostrach, An analysis of laminar free convection flow and heat transfer about a flat plate parallel to the direction of the generating body force, NACA TR 1111 (1953).
7. S. V. Patankar and D. B. Spalding, A finite difference procedure for solving the equations of the two dimensional boundary layer, *Int. J. Heat Mass Transfer* **10**, 1389–1411 (1967).
8. R. J. Moffat and W. M. Kays, The turbulent boundary layer on a porous plate: experimental heat transfer with uniform blowing and suction, *Int. J. Heat Mass Transfer* **11**, 1547–1566 (1968).
9. R. Ladenburg and D. Bershader, *Physical Measurements in Gas Dynamics and Combustion*, Vol. IX, pp. 47–75. Princeton Series in High Speed Aerodynamics and Jet Propulsion (1954).
10. W. Hauf and U. Grigull, Optical methods in heat transfer, in *Advances in Heat Transfer* Vol. 6, pp. 133–366. Academic Press, New York (1970).

CONVECTION NATURELLE SUR UNE PLAQUE POREUSE VERTICALE AVEC TRANSPIRATION

Résumé—On étudie numériquement et expérimentalement le problème de la convection naturelle sur une plaque poreuse, verticale et isotherme, avec transpiration. On dégage l'effet de la transpiration uniforme sur le transfert thermique et sur la température. Un bon accord est observé entre le calcul et les mesures interférométriques des profils de température adimensionnelle pour des valeurs

$$\xi \triangleq \frac{v_0 x}{\nu}\left(\frac{4}{Gr_x}\right)^{1/4}$$

comprises dans le domaine $-2 \leqslant \xi \leqslant 2$. La précision de la mesure du profil de température est estimée à $\pm 0{,}55$°C pour $(T_W - T_\infty) = 28$°C.

FREIE KONVEKTION UND VERDUNSTUNG AN EINER SENKRECHTEN PORÖSEN PLATTE

Zusammenfassung—Das Problem der freien Konvektion an einer isothermen, senkrechten porösen Platte mit Verdunstung wird numerisch und experimentell untersucht. Die Einflüsse der gleichmäßigen Verdunstung auf die Wärmeübertragung und die Temperatur- sowie Geschwindigkeitsprofile werden bestimmt. Experimentelle, interferometrisch gewonnene Daten von dimensionslosen Temperaturprofilen für Werte der Variablen

$$\xi \triangleq \frac{v_0 x}{\nu}\left(\frac{4}{Gr_x}\right)^{1/4} \quad \text{im Bereich} \quad -2 \leqslant \xi \leqslant 2$$

zeigen eine gute Übereinstimmung mit den numerisch erhaltenen Werten. Bei der Bestimmung der Temperaturprofile für $(T_w - T_\infty) = 50$°F wird eine Unsicherheit von ± 1°F veranschlagt.

СВОБОДНАЯ КОНВЕКЦИЯ ОКОЛО ВЕРТИКАЛЬНОЙ ПОРИСТОЙ ПЛАСТИНЫ ПРИ ПОРИСТОМ ИСПАРЕНИИ

Аннотация — В данной работе численно и экспериментально изучается свободная конвекция около изотермической вертикальной пористой пластины при пористом испарении. Рассчитываются профили температуры и скорости, а также влияние однородного пористого испарения на перенос тепла. Полученные интерферометрически экспериментальные данные по безразмерным температурным профилям для значений переменной $\xi \triangleq \frac{v_0 x}{\nu}\left(\frac{4}{Gr_x}\right)^{1/4}$ вдоль по потоку в диапазоне $-2 \leqslant \xi \leqslant 2$ хорошо согласуются с результатами расчётов. При измерении профиля температуры для $(T_w - T_\infty) = 50°$ F получена точность в $\pm 1°$ F.